electronics

MDPI

Article

Proposal of an External Remote Sensing Circuitry for Switching-Mode Power Supplies

George Catalin Salavarin [1,2], Vlad-Mihai Placinta [1,*] and Cristian Ravariu [2]

[1] Department of Elementary Particle Physics, Horia Hulubei National Institute for R&D in Physics and Nuclear Engineering (IFIN-HH), 077125 Magurele, Romania
[2] Faculty of Electronics, Telecommunication and Information Technology, National University of Science and Technology Politehnica Bucharest (UNSTPB), 060042 Bucharest, Romania
* Correspondence: vlad-mihai.placinta@cern.ch

Abstract: This work proposes a low-cost and easy-to-implement solution for a remote voltage-sensing circuitry that can be used to ensure stability and good voltage regulation in applications with power supplies driving currents over long paths. The circuitry is implemented with general-purpose electronic components and is provided as an external feature to be attached to power supplies without remote sensing. To demonstrate its capabilities, a test bench was put together alongside a power supply module which has local sensing only. With the test bench, the output voltage from the power supply was delivered in various scenarios to an electronic load. Multiple parameters were monitored in order to assess the power supply performance to which the proposed remote voltage-sensing circuitry is attached. The measurements include stability and transient response tests, and the results were compared with the ones obtained with the standard local sensing. The tests reveal that the power supply module kept its output voltage stable with less than +/−10% voltage variation, and the average transient recovery time was less than 100 µs. The results are given for two different output voltage values of 1.2 V and 3.3 V and at high current capabilities of 3.5 A.

Keywords: switching-mode power supply; remote voltage-sensing feedback; low-voltage applications

check for updates

Citation: Salavarin, G.C.; Placinta, V.-M.; Ravariu, C. Proposal of an External Remote Sensing Circuitry for Switching-Mode Power Supplies. *Electronics* **2024**, *13*, 2994. https://doi.org/10.3390/electronics13152994

Academic Editor: Esteban Tlelo-Cuautle

Received: 13 June 2024
Revised: 23 July 2024
Accepted: 27 July 2024
Published: 29 July 2024

Copyright: © 2024 by the authors. Licensee MDPI, Basel, Switzerland. This article is an open access article distributed under the terms and conditions of the Creative Commons Attribution (CC BY) license (https://creativecommons.org/licenses/by/4.0/).

1. Introduction

The performance of the switching-mode power supplies in modern electronic designs is a key factor in ensuring a reliable operation of a user system. The current state of the art provides very efficient and integrated power supply regulators with only a few external components required for operation. The reference designs provided by the vendors cover most of the user needs in terms of powering in applications. However, there are a few applications in which most of the commercial power circuits cannot be used as standalone circuits. This particular case is related to remote-powering applications, in particular, to the ones requiring remote sensing capabilities to compensate for the voltage drops. Usually, these remote-powering applications are required when the power supply and the user system cannot be in the same place and close to each other due to various application-related constraints. Such applications can be remote instrumentation applications and radiation testing of integrated electronic circuits such as in [1] and nuclear power plants.

The market availability is not so good for multi-channel power supply circuits with remote sensing capabilities embedded in the same package. Obviously, the main reasons for this are higher costs and because they have limited support, in some cases, for multi-channel configuration. Therefore, conventional power circuits with local sensing are preferred due to their large variety and availability on the market in different configurations. In this case, the reference design needs to be adapted to work in the remote sensing mode. Generally, there are three main types of sensing in a power supply: local sensing, partial remote sensing, and full remote sensing [2].

Local sensing is the most common as well as the simplest mode to use, as it is available by default in the majority of the market's power supply circuits. When operating in this mode, the power supply regulates the output voltage only around its output pins (more precisely, the junction of the output voltage and the feedback pin), and therefore there is no mitigation on possible voltage drops. In this mode, it is expected that the load is placed very close and near the outputs of the power supply, thus resulting in insignificant voltage drops. However, when using long paths to deliver the power to the load, there will be significant voltage drops across the path directly related to the current consumption by the load. This makes this sensing configuration not suitable for use in a remote-powering application that requires stable voltages for the load.

A way to enhance the voltage regulation and to reduce the voltage drops is to move the feedback pin connection near the load. This is called partial remote sensing and can help to reduce voltage drops by half. The other half is given by the different voltage levels of the grounds between the power supply and the load, which, in this case, cannot be mitigated. This is mainly due to the fact that there is no feedback pin to also sense the ground on the load side.

Full remote sensing represents the best choice to mitigate voltage drops across long paths when the power supply is not located near the load. In this configuration, the voltage across the load is sensed on both the positive and ground sides, resulting in very low voltage drops. However, this method involves two additional wires for sensing and for power supply circuits without remote sensing capabilities and it requires additional external circuitry.

At the time of writing this paper and to our knowledge, there are not many solutions available on the market to implement this feature as a plug-in for power regulators without remote sensing capabilities. One solution which we found is the LT4180 circuit [3] from Linear Technology (now Analog Devices). This circuit interrogates the line impedance and adjusts the voltage on the feedback pin based on the impedance variations [4]. This approach removes the need for additional wires used for remote sensing as it can be placed on the same board with the power supply. However, it has several limitations like minimum voltage sensed is 3.1 V, high complexity, large package (SSOP-24), and support for only one power supply channel per package. Apart from LT4180, there are only dedicated power regulators with integrated remote sensing capabilities and usually with a limited number of output channels. Some examples of such circuits are MAX8952 [5], MAX20830 [6], LT7170 [7], and SiC450 [8], and all of them have only one output channel.

With the above-mentioned limitations, it becomes a complex job to design a small and low-cost multi-channel power supply unit that can be used in remote-powering applications for field programmable gate arrays (FPGAs) or application-specific integrated circuits (ASICs). In such applications, multiple power rails are required, usually with low-voltage outputs and high-current capabilities such as 1 V, 1.5 V, 1.8 V, 3.3 V, and 5 V [9]. In terms of stability, it is desirable that the maximum output variation should be within $+/-10\%$, while the transient recovery time should be less than 100 µs on average for an output voltage between 1 V and 3.3 V and for an average load step of 1 A/µs.

This paper proposes an alternative solution to the LT4180 integrated circuit that can be attached as an external circuitry to enable remote voltage-sensing capabilities to a broad range of switching mode power supplies that do not have this feature by default. The proposed circuitry relies on a unity-gain differential amplifier used to read out the voltage across the load and to drive the single-ended feedback pin of the power supply output channel. It is intended to be placed on the same board with the power supply module, thus requiring only two screened wires to provide a readout of the voltage across the load to the circuitry. When compared to the other solution, the main advantages are visible mostly in the implementation, as the proposed solution is low-cost and easy-to-implement. Another major gain is the minimum voltage that can be sensed, as it can go as low as below 1 V if required, while the LT4180 solution can only work with 3.1 V as the minimum voltage that can be sensed and regulated. In terms of the space occupied, the proposed solution fits well

in a space-constrained design, as it requires up to eight components to implement remote sensing for one output channel. This can be helpful to apply on all the output channels of a multi-channel power supply module, while keeping everything on a small occupied area.

This remote voltage-sensing circuitry has already been validated and tested in its early iterations in various remote-powering applications involving radiation testing of FPGAs [10–12].

2. Test Bench Architecture and Testing Methodology

Generally, most of the power regulator families have only local sensing capabilities. They operate by regulating the output voltage with respect to a voltage that is read on the single-ended feedback pin. This method works well if the load is placed very close the output of the power regulator, as shown in Figure 1a. However, to be able to use the same power regulator to supply a load placed at a farther location, special attention must be given to the feedback loop in order to compensate for the voltage drops across the resistive path. To cope with this requirement, we propose an external remote feedback circuitry that can be used to track the voltage across the load and help the power regulator to maintain a stable output voltage, within the limits, to the load. Figure 1b shows the diagram of how we intend to use our solution to implement remote sensing capabilities to a power regulator which does not support this by default.

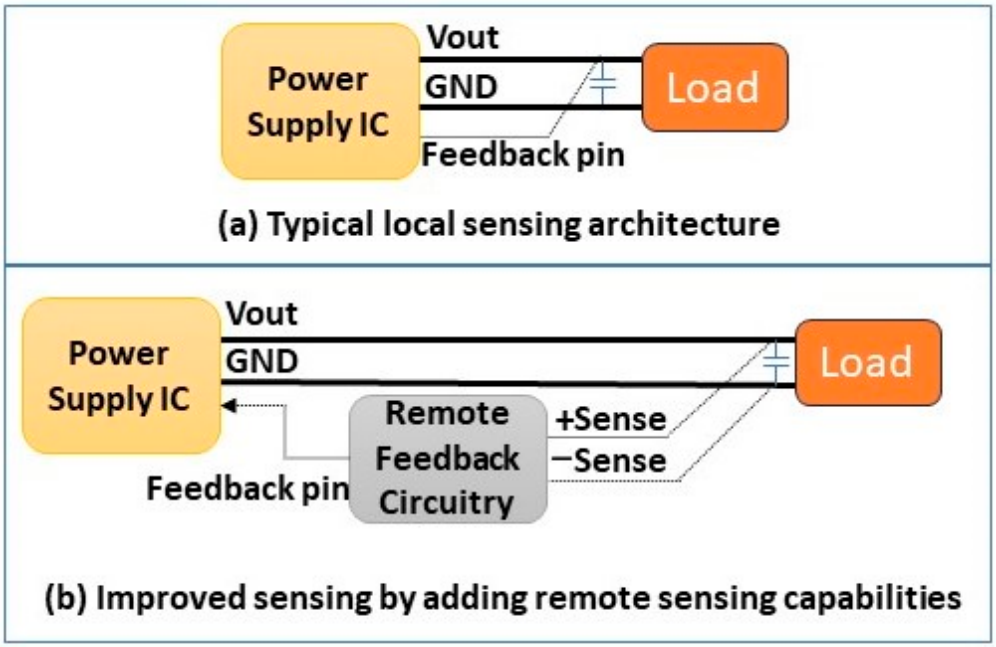


Figure 1. (**a**) Typical local sensing for a power regulator with single-ended feedback pin; (**b**) enhanced sensing with remote sensing capabilities for a power regulator with single-ended feedback pin.

To demonstrate and test the capabilities of the proposed remote voltage-sensing circuitry, a test bench was put together. Its architecture is depicted in Figure 2, and it basically contains the following components: a microcontroller-based carrier board, a multi-channel power supply module (PSM from now on), a simple board that is used to simulate the load behavior being connected to an electronic load, and a GUI (graphical user interface) to be able to control a monitor the tests.

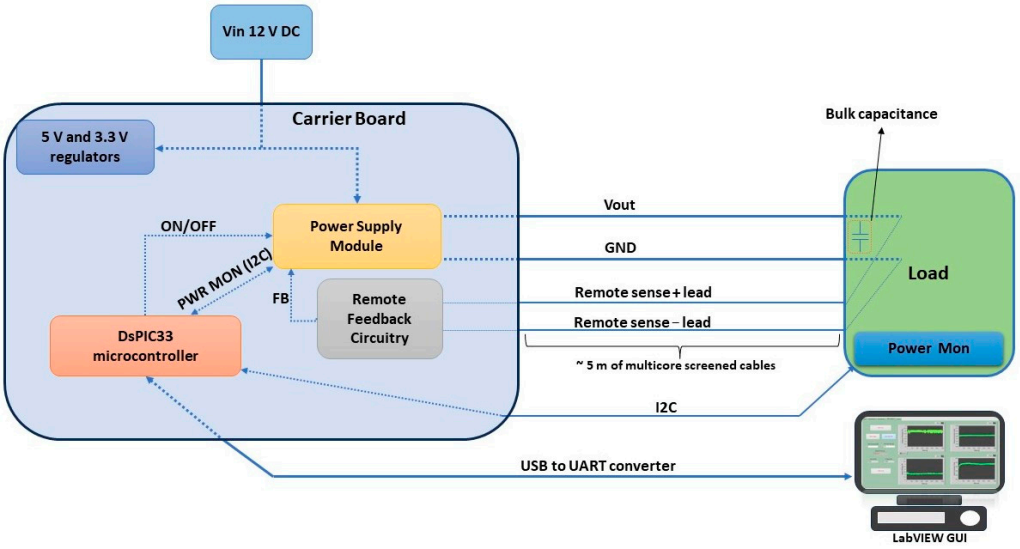


Figure 2. Block diagram of the test bench used to assess the performance of the proposed remote voltage-sensing circuitry.

The carrier board was designed to host the PSM in a plug-and-play manner. It relies on DsPIC33EP512MU810 [13] microcontroller to implement various functions and controls and to enable full monitoring of the test bench. The design of the carrier board is rather simple, and apart from the microcontroller and all of its additional circuits needed to operate, it also embeds the remote voltage-sensing circuitry that is proposed in this study.

The output voltages from the PSM channels were routed through the carrier board and delivered with 5 m of multicore screened cables to a simple board which played the role of an actual load placed at a farther location with respect to the PSM output. An electronic load was connected to this board to act as a load to the PSM output. There was some bulk capacitance on the board placed near the joint connections to the electronic load. The capacitance is mandatory to ensure the stability of the PSM control loop by filtering out the additional noise which may be induced by the long wires as well as by acting as a reserve of charge in high-current modes. It has the possibility to monitor the realistic voltage and the current consumption across the load. These were measured by using INA219, a dedicated I2C-based power monitor [14]. A benchtop commercial electronic load was used to simulate the behavior of an actual load in various scenarios such as high-load or transient-load modes. The electronic load was controlled by using the GUI and was set to work in the constant-current (CC) mode.

The control loop of the PSM output channel was fed with a voltage that tracks the actual voltage across the load located farther away. This was accomplished by using the circuit architecture presented in Figure 3. It relied on a unity-gain and non-inverting differential amplifier that was used to read the voltage across the load through 2 screened cables. Due to its unity-gain design, the output voltage (V_{out}) of the amplifier tracked the input voltage difference across its inputs (V_1 and V_2). Then, the V_{out} was used to drive the voltage divider of the PSM control loops (feedback pin). In this way, the PSM did not know if the feedback voltage came for local sensing or via the long cables. It regulated its output voltage across the load to match the required voltage set by the voltage divider ratio.

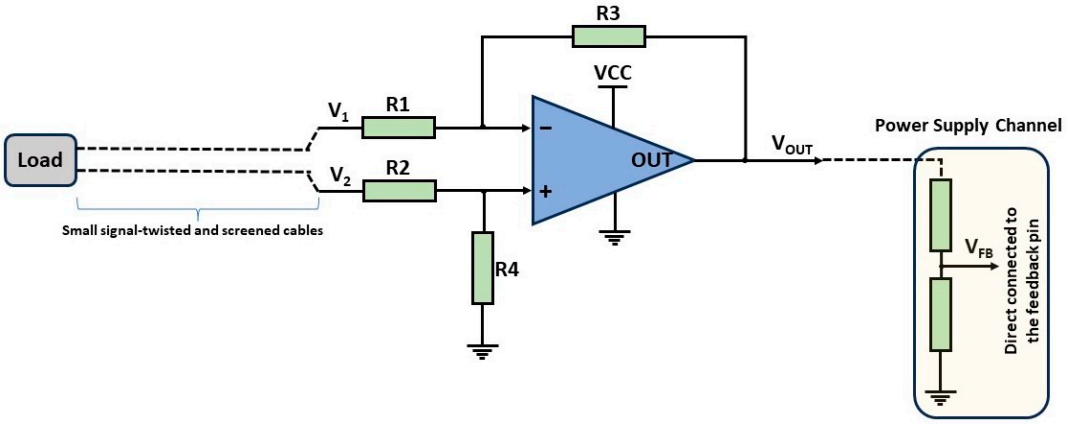


Figure 3. The remote voltage-sensing circuitry architecture implemented with unity-gain differential amplifiers. This is represented only for one output channel of the PSM.

When designing such circuits, there are a few things to take into account to minimize errors and to maintain the output voltage. The first step is choosing the operational amplifier. In Table 1, there is a short list with the parameters of interest which need to be considered when selecting the operational amplifier. The list is not exhaustive, and there are many options available on the market from different vendors and at a reasonable price. Additionally, all 4 resistors, R1–R4, should have the same value and very good precision. For this study, we used resistors with 1000 Ω resistance and with 1% precision. This will enhance the precision of the nominal output voltage of the PSM and eliminate the need for using multi-turn trimmers for fine-tuning the output voltage.

Table 1. List of minimum requirements that need to be considered when choosing an operational amplifier for use with the proposed remote voltage-sensing method.

Parameter	
gain bandwidth product (GBWP)	better than 1 MHz
common-mode input voltage	rail-to-rail *
output swing	rail-to-rail *
slew rate	better than 0.1 V/µs
input bias currents	FET-based inputs
input offset voltage	maximum +/−10 mV
power supply	single power supply operation

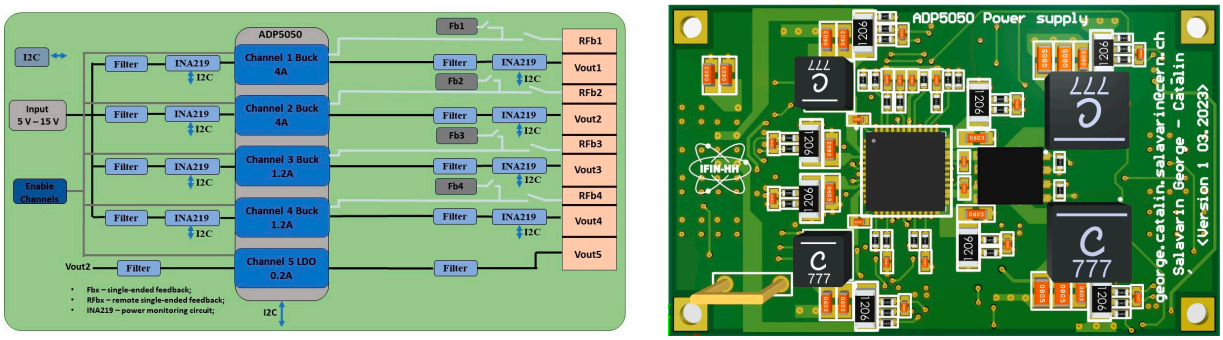
* The actual range may vary for different vendors or operational amplifier families.

For the tests that are presented in this paper, an operational amplifier from the MCP6001/2/4 family [15] was chosen. This part number fits well with the parameters from the list presented in Table 1. According to the datasheet, the input offset voltage is in the range of +/−4.5 mV, while the input bias current values are within the range of +/−1 pA, for normal operating conditions. These parameters play an important role in maintaining the accuracy of the voltage tracking. Larger values of these parameters can contribute to large variations in the regulated voltage. Single-supply operation mode with the operational amplifier powered with 5 V was employed. The rail-to-rail input and output feature set a common-mode input range (V_{CMR}) between "V_{SS} − 0.3 V" and "VDD + 0.3 V". This allowed to test a broad range of standardized PSM output voltages between the range of 1 V and 3.3 V.

The impact of the twisted cables on the variation in the output voltage is negligible, as they have small resistance and the input bias currents of the operational amplifier are very small. The cables were screened to the ground to further enhance the overall stability of the PSM control loop by eliminating any noise that can disturb the voltage regulation.

All the tests that were carried out in this paper to demonstrate the capabilities of the proposed remote voltage-sensing method, were performed with a PSM designed around the ADP5050 [16] multi-channel power supply integrated circuit. This circuit embedded 4 switching mode and high-current output channels and an additional small-current linear regulator. Only one switching mode output channel was used for this work.

The PSM that is shown in Figure 4 is designed on a 4-layer PCB with 50 mm × 25 mm dimensions. It embeds the possibility of measuring the voltage and the current on every power channel on both input and output sides. This was implemented with INA219 circuits. Additionally, the sensing mode can be switched individually from local sensing to fully remote sensing with the help of 0-ohm resistors. The operating frequency was set to 600 KHz, and the components were chosen accordingly to the datasheet guidelines and depending on the output voltage configuration. The module was connected to the carrier board through header connectors and enforced by four mounting holes in each corner. The carrier board provided the input voltage, which was split on the PSM side for every power channel. An I2C interface was available for reading out the power measurement circuits, as well as to configure the ADP5050 circuit, if needed. The possibility to individually enable or disable different output channels was also implemented. On the PSM, local sensing was connected to the output voltage after the shunt resistors that was used for measuring the current consumption. However, when using remote sensing mode, the voltage that needed to be regulated came from the remote voltage-sensing circuitry that was placed on the carrier board.



(**a**) (**b**)

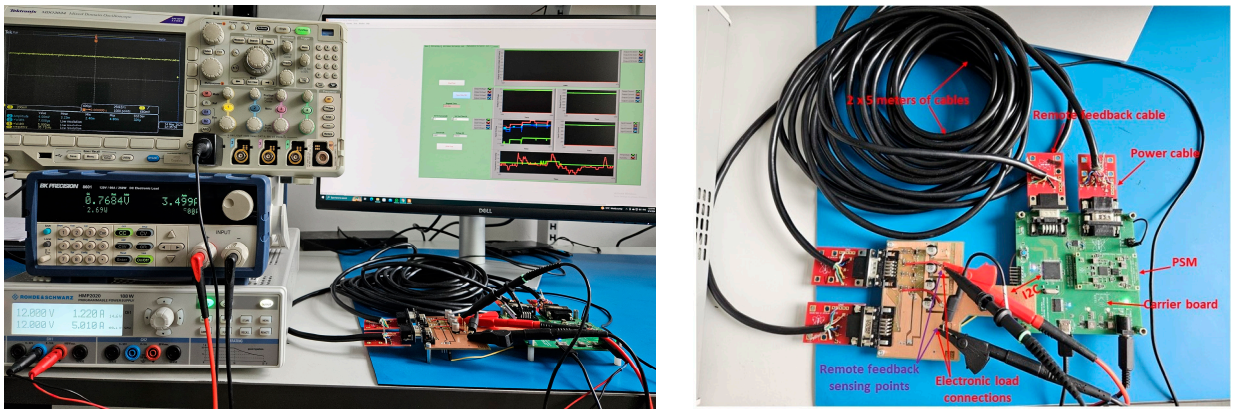
Figure 4. Multi-channel power supply module designed around ADP5050: (**a**) schematic diagram which shows all of its features; (**b**) 3D view of the implementation.

The entire test bench along with the electronic load were connected to a LabVIEW™-based GUI. From this GUI, the user can control everything and can monitor in real time the measurements on various graphs. Additionally, the data were saved in files for later analysis.

Testing Methods

Figure 5 shows the entire test bench implementation that was used to perform the measurements and to analyze the efficiency of the proposed remote voltage-sensing circuitry. The output voltage from one channel of the PSM was delivered to the electronic load. The only difference is where the load was placed. When using local sensing, the load was located very close to the output of the PSM, while in remote sensing mode, the load was located after 5 m of cables. The remote feedback circuitry senses the voltage across the electronic load in the point that is labelled with "remote feedback sensing points" in Figure 5b. The INA219 power monitors allow to measure the voltage with 4 mV/LSB, while the current is measured with 200 µA/LSB. Every measurement point for both voltage and the current is an average of 32 samples, which were taken in ~17 ms. The bulk capacitance on the electronic load side is 2 × 470 µF (electrolytic type). The 5 m of cable has an equivalent inductance of ~10 µH and a resistance of 0.5 ohms. The cable and the additional bulk capacitance form a parasitic LC filter, which can modify to some extent

with the transient recovery time of power regulator. Otherwise, it should not have much of an impact on the performance of the power regulator.



(**a**) (**b**)

Figure 5. Test bench implementation: (**a**) view from the front with all the tools and apparatus involved in the tests including the LabVIEW GUI in the background; (**b**) detailed picture of the components.

Several methods were used in this paper to validate the performance of the proposed remote voltage-sensing circuitry in different scenarios. All the measurements are given with respect to the standard local sensing scenario in Section 3.

A first test was performed to check the stability of the output voltage over a longer period of time and at a high and constant output current. The purpose of this test was to check that the output voltage variation stays within +/−10% and there were no oscillations present on it. Also, this test can give an idea if the control loop suffers instabilities due to the additional parasitic LC filter and the external circuitry involved in the voltage regulation.

Then, the tests can be modified so that the load can draw different values of currents in steps to check the response of the power regulator. In this way, the load was configured to generate step current increases from minimum to maximum values of current and vice-versa. Each step had similar times and amplitudes. These tests were useful to check the dynamic response of the control loop and to assess if the output stability was within the boundaries and that there were no instabilities caused by the step increases or decreases in the current with respect to the local sensing mode.

Transient tests with the load configured to switch from 0 to a maximum current value and at a given time interval were also a good test to validate the overall stability of the power regulator in remote sensing mode. Although it is a harsh working regime for a power regulator, it can withstand any problems and instabilities in the control loop of the power regulator that can be induced by the additional parasitic LC filter and the remote sensing circuitry. Also, when discussing transient tests, some measurements with an oscilloscope for the transient response of the power regulator are mandatory. The measurements are to be compared with the simulated results, for this particular case.

In this paper, only the tests carried out for one output channel ("channel 1" from Figure 4) of the PSM are given, as all the channels should behave in the same way. The measurements were taken only for 2 output voltage values: 1.2 V and 3.3 V. These two values are among the most common ones in modern electronics; hence, it may help the user to extrapolate the behavior to other output voltages between these 2 values and beyond. The maximum current of the output channel was set to 3.5 A.

3. Experimental Data and the Results

The first tests were carried out to demonstrate the PSM output voltage stability at a high and constant load when using the proposed remote voltage-sensing circuitry. The measurements were taken over 1 h of operation for both sensing modes for comparison. A summary of the results of this test is given in Table 2 and highlights very good stability of the power regulator when coupled with the remote voltage-sensing circuitry. From the table, it can be observed that the variation is well below +/−10%, which represents the maximum that can be admitted with respect to the nominal voltage.

Table 2. Stability test results of the power regulator at a high and constant load of 3.5 A when set to 1.2 V and 3.3 V outputs and by using both sensing modes: local and remote sensing.

Nominal Voltage Set	Variation When Using Local Sensing [%]	Variation When Using Remote Sensing [%]
1.2 V	<+/−0.1%	+/−0.9%
3.3 V	<+/−0.1%	+/−0.4%

The next step in the validation was to test the circuitry with a variable load. The test started from a baseline current of 0.5 A that was increased by 0.5 A at every 30 s until it reached the maximum current of 3.5 A. Once the maximum current was touched, the load was decreased in the same way with 0.5 A at every 30 s, until it reached the baseline value again. Figures 6 and 7 show the stability of the PSM output voltage when using both sensing modes and with the output voltage set to 1.2 V and 3.3 V. The measurements presented on the left side of the figures are compared with the ones taken with the standard local sensing mode and are given on the right side. From Figure 6, it can be observed that the PSM regulates the 1.2 V output voltage quite well with both sensing modes, highlighting the very good stability in both cases and at a variable load. For the 3.3 V case and using the remote voltage-sensing mode, the measurements that are given in Figure 7a reveal a variation of about +/−10 mV. This represents a variation of ~+/−0.3% from the nominal value.

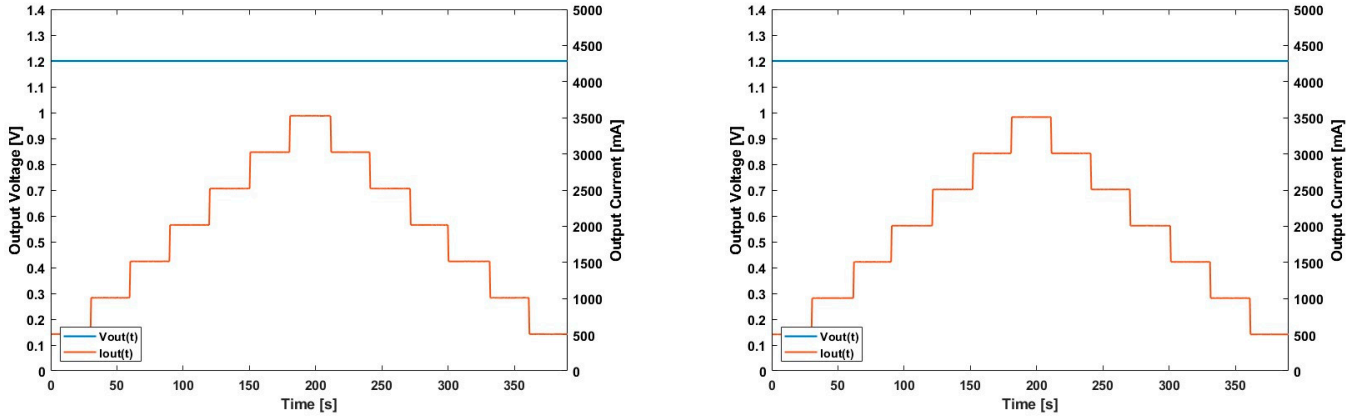


Figure 6. PSM stability tests with an output voltage set to 1.2 V and current drawn by the load being increased in steps of 0.5 A until it reaches 3.5 A and then decreased in the same steps: (**a**) results with remote voltage-sensing mode: no variations with respect to the nominal voltage of 1.2 V; (**b**) results with local sensing on the PSM side: no variations with respect to the nominal voltage of 1.2 V.

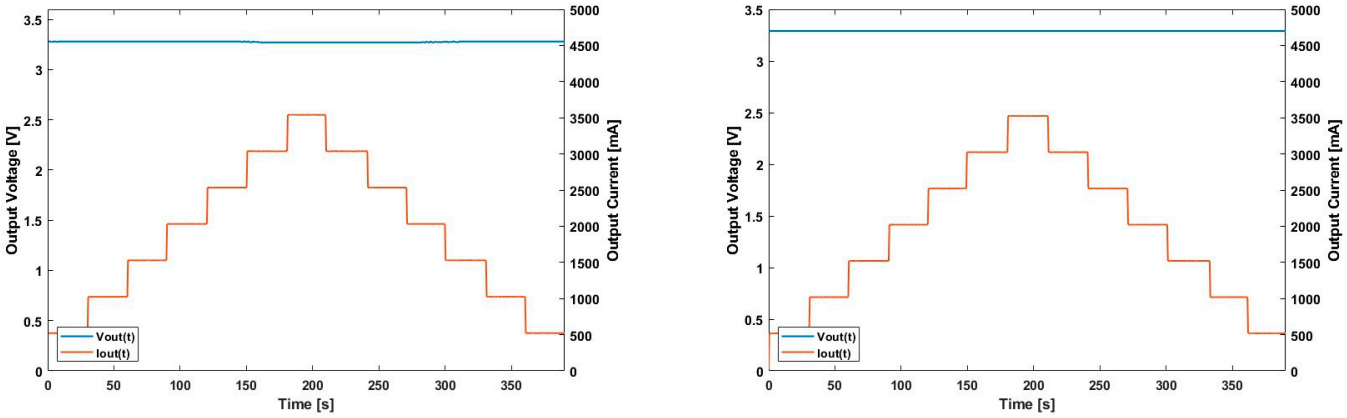


Figure 7. PSM stability tests with an output voltage set to 3.3 V and current drawn by the load being increased in steps of 0.5 A until it reaches 3.5 A and then decreased in the same steps: (**a**) results with remote voltage-sensing mode: nominal = 3.29 V; minimum = 3.27 V; maximum = 3.28 V; and average = 3.275 V; (**b**) results with local sensing on the PSM side: no variations with respect to the nominal voltage of 3.29 V.

To highlight further the performance of the proposed remote voltage-sensing circuitry when connected to the PSM, another set of tests which consisted of repetitive transient current variations between the minimum and the maximum values was employed. For both values of 1.2 V and 3.3 V as the output voltages, the current drawn by the electronic load was switched between 0 and 3.5 A every 10 s. The results are presented in Figure 8, and the data show variations of +/−0.83% for the 1.2 V output and 0.6% for the 3.3 V output. Also, in Figure 8a, a small drop in the voltage is noticed when the current is 0, and the amplitude is 10 mV; this is mainly due to the overcompensation of the remote feedback circuitry as it tries to match the voltage across the load quite fast when the load is transient and under these harsh conditions. This effect is mainly due to the differential amplifier operation, and it should not impact the load, as the amplitude variation is well below the +/−10% limit.

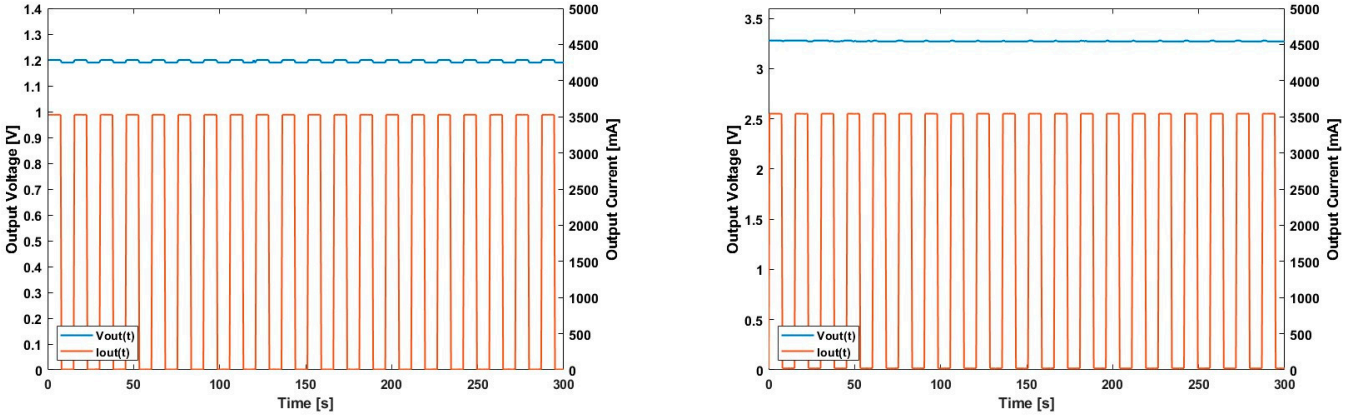
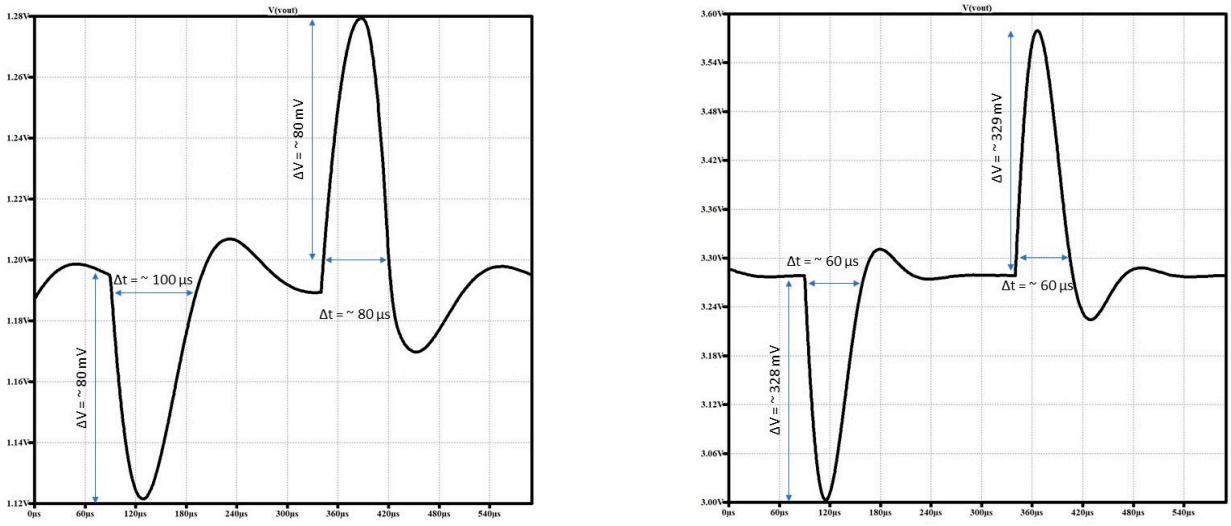


Figure 8. PSM stability tests performed when using the remote voltage-sensing circuitry and with a repetitive transient load. The current drawn by the load was switched between 0 and 3.5 A at a given time interval of 10 s: (**a**) results with output voltage set to 1.2 V: nominal = 1.2 V; minimum = 1.19 V; maximum = 1.2 V; and average = 1.195 V; (**b**) results with output voltage set to 3.3 V: nominal = 3.29 V; minimum = 3.26 V; maximum = 3.29 V; and average = 3.275 V.

From the measurements, it can be deduced that the undershoots and the overshoots were kept to minimum for two reasons. One reason is the acquisition time of ~17 ms for every point that contains an average of 32 individual samples which may filter them out, if they have a shortened time. Another reason is the parasitic LC-type filter formed by the long cable and the bulk capacitance. The inductance of the cable was measured to be around 10 µH, and this helped to limit the current flow to the load and reduce the current ripple. This led to a slower transient recovery time, but a better voltage ripple and a good voltage stability. The tests reveal that the stability of the PSM control loop is not affected by the additional parasitic LC filter.

The evaluation was concluded with some transient response measurements that were taken for both output voltages and with both sensing modes. The measurements were taken with an oscilloscope set in the "AC-coupling" mode. The load was switched from 20% to 80% (0.8 A to 3.2 A) and vice-versa in all the cases. The slew rate of the electronic load was set to 2.5 A/µs. Therefore, the contribution of the electronic load to transient recovery time is negligible.

Simulations were carried out before the actual experimental data taking. The results are given in Figure 9 for both output voltage values and when using the remote voltage-sensing circuitry. The simulation also included the parasitic LC filter formed by a 10 µH inductor and 2 × 470 µF.

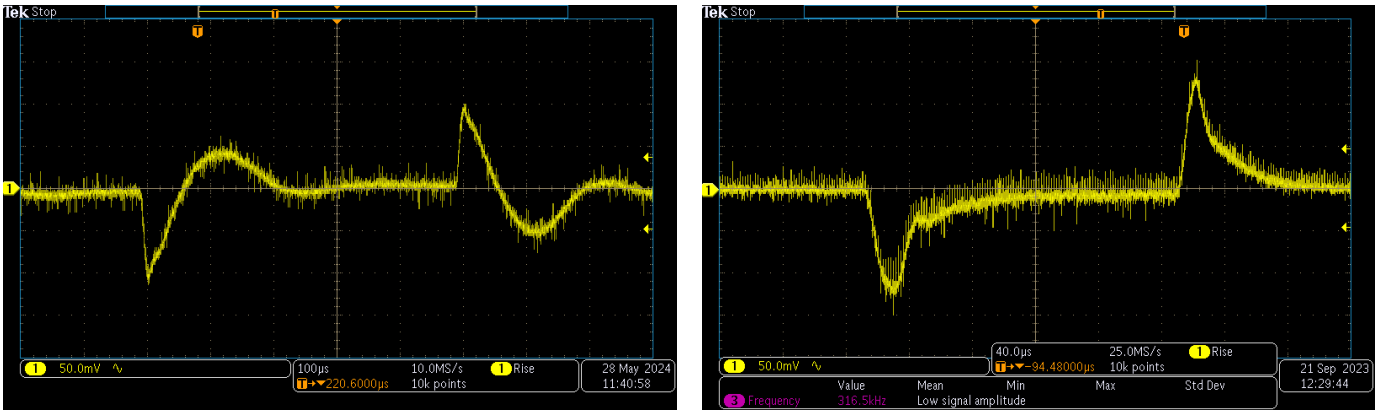


(**a**) (**b**)

Figure 9. Simulations results of the transient response of the PSM when using the remote voltage-sensing circuitry and with different output voltages. The load was switched from 20% to 80% and vice-versa: (**a**) results with output voltage set to 1.2 V: overshoot/undershoot amplitude = ~+/−80 mV (~+/−7%), time = ~100 µs; (**b**) results with output voltage set to 3.3 V: overshoot/undershoot amplitude = ~+/−328 mV (~+/−10%), time = ~60 µs.

Figure 10 shows the transient response measurements taken with the output voltage set to 1.2 V. The baseline values of the transient response parameters are given in Figure 10b and were measured with a local sensing mode and with standard values of the components. The maximum variation in overshoot/undershoot was determined to be ~+/−125 mV, which can be translated to a ~+/−10% variation. The transient recovery times for both overshoots and undershoots are roughly ~60 µs. However, as expected, and mostly due to the bulk capacitance placed near the load, when using the remote voltage-sensing mode, the transient response is different with respect to the measurements that were taken using the local sensing mode. It was measured that the amplitude of the overshoots and undershoot was reduced to ~+/−100 mV (+/−8% variation), while the transient recovery time now increased to ~100 µs. Additionally, as can be seen in Figure 10a after the undershoot, there is

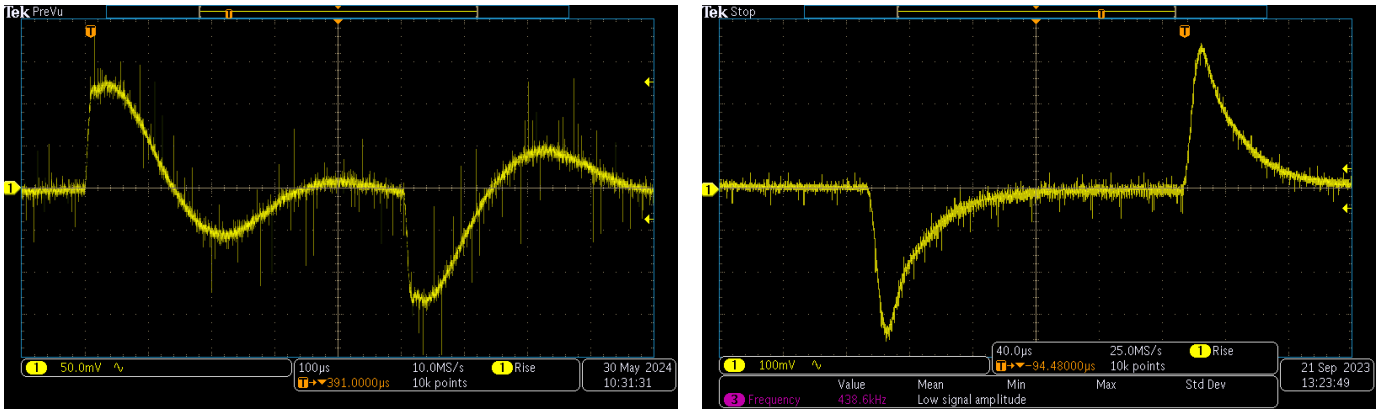
a small oscillation present which is self-mitigated after a short time, with the output voltage being stable. This was also confirmed by the simulation and may be further prevented or adjusted with some modifications of the PSM compensation network. However, this is not covered in this paper, as we believe that for most of the applications which are based on this ADP5050 integrated circuit, the compensation network can remain the same as it is set by default with the design values provided by the vendor.



(**a**) (**b**)

Figure 10. PSM transient response measurements for both sensing modes with the output set to 1.2 V and the load being switched from 20% to 80% and vice-versa: (**a**) results with remote voltage-sensing mode: overshoot/undershoot amplitude = ~+/−100 mV (~+/−8%), time = ~100 µs; (**b**) results with local sensing mode: overshoot/undershoot amplitude = ~+/−125 mV (~+/−10%), time = ~60 µs.

Similar results were also measured for the 3.3 V set as the output voltage. Figure 11 shows more or less the same behavior of the PSM control loop. The overshoot/undershoot amplitudes were reduced by 65%; however, the transient time increased by almost 90%, when compared with the values measured in the local sensing mode. This is again mainly due to the additional bulk capacitance and the inductance created by the long cables.



(**a**) (**b**)

Figure 11. PSM transient response measurements for both sensing modes with the output set to 3.3 V and the load being switched from 20% to 80% and vice-versa: (**a**) results with remote voltage-sensing mode: overshoot/undershoot amplitude = ~+/−125 mV (~+/−4%), time = ~150 µs; (**b**) results with local sensing mode: overshoot/undershoot amplitude = ~+/−350 mV (~+/−10%), time = ~80 µs.

The tests and the measurements show that this remote voltage-sensing circuitry can be used with power regulators to implement remote sensing capabilities. However, several factors have to be taken into consideration: the bulk capacitance should not be large, as it can further degrade the transient response, and the long cables need to have small resistance and inductance as this can have a big influence on the stability of the power regulator. Overall, the results show a good stability well within +/−10% acceptance. Its simplicity and small occupied area per channel also offer the possibility to be used on low-voltage values (e.g., 1.2 V), or even lower, making it a good candidate and a viable solution to be taken into consideration for designs requiring remote powering.

4. Conclusions

In this paper, we propose a low-cost and easy-to-implement remote voltage-sensing circuitry that can be used to add remote sensing capabilities to power regulators which do not have this feature by design. The circuit is implemented with general-purpose components that have reasonably low acquisition costs. Overall, on the market, there are not may solutions that can fulfill this need, as the only solution that we found is LT 4180. This is a dedicated virtual remote sensing circuit that can perform the same way as our proposed solution. However, the main drawbacks are SSOP24 package supports only one channel, multiple components needed, minimum voltage sensed is 3.1 V, and overall high acquisition price (~ EUR 10). Our solution uses up to eight components, and the total cost does not exceed EUR 2. Due to the small footprint, it occupies a small area on the PCB and it can be used in multi-channel power rail configurations in space-constrained designs. Also, we demonstrate in this paper that it can be used to sense voltages as low as 1.2 V, and even lower.

The measurements that were carried out in this paper to validate this remote voltage-sensing circuitry show very good results in terms of stability over time as well as transient response. With the test bench that was described in this paper, it showed improvements in the overshoots/undershoots caused by the transient load and some degradations of the transient recovery time. The overall voltage variation from the nominal voltage was measured to be within the +/−10% boundary, while the maximum transient recovery time was measured to be ~100 µs. These values are not so restrictive and should not impact most of the load.

The proposed remote voltage-sensing circuitry represents a viable option to implement such a feature to a power supply providing a good compromise in terms of stability, voltage regulation, and transient response. Previous iterations have been already validated by our group in various remote-powering applications for FPGAs and other complex integrated circuits.

As future work, we plan to extend the testing of this circuitry to other scenarios and with different voltage regulators such as linear type or other types of DC–DC converters. We also want to improve the transient response by redesigning the compensation network to also account for the parasitic LC filter and the additional circuitry.

Author Contributions: G.C.S. and V.-M.P. equally contributed to this research starting with the concept, hardware, test bench implementation, data acquisition, and data analysis, as well as the preparation of this paper. C.R. contributed by reviewing the paper, discussing the methodology, and analyzing the results, which helped to significantly improve the quality of the paper. All authors have read and agreed to the published version of the manuscript.

Funding: The research as well as all the preparation, materials, and the apparatus that were used to carry out these studies were supported by the Ministry of Research, Innovation and by the Institute of Atomic Physics Bucharest (IFA) through LHCb-RO grant number 5/03.01.2022 and the national project "NUCLEUS", grant number PN 23 21 01 04.

Data Availability Statement: Data are contained within this article.

Conflicts of Interest: The authors declare no conflicts of interest.

References

1. Tian, J.; Cao, R.; Liu, Y.; Cai, Y.; Mei, B.; Zhao, L.; Cui, S.; Lv, H.; Xue, Y. Electron-Induced Single-Event Effect in 28 nm SRAM-Based FPGA. *Electronics* **2024**, *13*, 2233. [CrossRef]
2. Advanced Energy—Remote Sense Techniques Application Note AN1103. Available online: https://www.advancedenergy.com/getmedia/b1d5b72a-59df-4ccb-9b5d-aad2779c14c8/en-lv-remote-sensing-application-note.pdf (accessed on 16 July 2024).
3. Analog Devices—LT4180 Virtual Remote Sense Controller. Available online: https://www.analog.com/media/en/technical-documentation/data-sheets/4180fb.pdf (accessed on 16 July 2024).
4. Analog Devices, Sam Davis—Controller IC Eliminates Remote Sense Lines for Long Cable Runs. Available online: https://www.analog.com/media/en/technical-documentation/technical-articles/ltc%20sam%20davis%20feature%20from%20may%202010%20pet.pdf (accessed on 16 July 2024).
5. Analog Devices—MAX8952 Datasheet. Available online: https://www.analog.com/media/en/technical-documentation/data-sheets/MAX8952.pdf (accessed on 16 July 2024).
6. Analog Devices—MAX20830 Datasheet. Available online: https://www.analog.com/media/en/technical-documentation/data-sheets/max20830.pdf (accessed on 16 July 2024).
7. Analog Devices—LT7170 Datasheet. Available online: https://www.analog.com/media/en/technical-documentation/data-sheets/lt7170-lt7170-1.pdf (accessed on 16 July 2024).
8. Vishay Siliconix—SiC450 Datasheet. Available online: https://www.vishay.com/docs/77863/sic450_sic451_sic453.pdf (accessed on 16 July 2024).
9. Khan, D.; Basim, M.; Ain, Q.u.; Shah, S.A.A.; Shehzad, K.; Verma, D.; Lee, K.-Y. Design of a Power Regulated Circuit with Multiple LDOs for SoC Applications. *Electronics* **2022**, *11*, 2774. [CrossRef]
10. Placinta, V.M.; Cojocariu, L.N.; Maciuc, F. A dedicated and versatile system for testing the radiation hardness of various integrated circuits. *JINST* **2023**, *18*, C01053. [CrossRef]
11. Placinta, V.M.; Cojocariu, L.N.; Maciuc, F.; Straticiuc, M.; Mattiazzo, S.; Silvestrin, L.; Candelori, A. Measurements of radiation effects in an antifuse FPGA. *Nucl. Instrum. Methods Phys. Res. Sect. A* **2023**, *1055*, 168551. [CrossRef]
12. Placinta, V.M. Complex Integrated Circuits in the Radiation Environment at the LHCb High Energy Physics Experiment and Extrapolation to the Case of Space-Based Experiments. Ph.D. Thesis, Polytechnic University of Bucharest, Bucharest, Romania, 2020.
13. Microchip—dsPIC33EPXXX(GP/MC/MU)806/810/814 and PIC24EPXXX(GP/GU)810/814 Datasheet. Available online: https://ww1.microchip.com/downloads/aemDocuments/documents/OTH/ProductDocuments/DataSheets/70616g.pdf (accessed on 7 June 2024).
14. Texas Instruments—INA219 Datasheet. Available online: https://www.ti.com/lit/ds/symlink/ina219.pdf?ts=1717691410326&ref_url=https%253A%252F%252Fwww.google.com%252F (accessed on 16 July 2024).
15. Microchip—MCP6001/1R/1U/2/4 Datasheet. Available online: https://ww1.microchip.com/downloads/en/DeviceDoc/MCP6001-1R-1U-2-4-1-MHz-Low-Power-Op-Amp-DS20001733L.pdf (accessed on 16 July 2024).
16. Analog Devices—ADP5050 Datasheet. Available online: https://www.analog.com/media/en/technical-documentation/data-sheets/ADP5050.PDF (accessed on 16 July 2024).

Disclaimer/Publisher's Note: The statements, opinions and data contained in all publications are solely those of the individual author(s) and contributor(s) and not of MDPI and/or the editor(s). MDPI and/or the editor(s) disclaim responsibility for any injury to people or property resulting from any ideas, methods, instructions or products referred to in the content.